

Structure design of gradient hard coatings on YG8 and their residual stress analysis by ANSYS^①

Song Huijin (宋慧瑾)^②, Yan Qiang^②, Dong Zhihong, Guo Wei, Tang Yirong
(College of Mechanical Engineering, Chengdu University, Chengdu 610106, P. R. China)

Abstract

A structure of gradient hard coatings (Ti, TiN, TiCN and TiAlN) is designed, and residual stress is simulated by a finite element method with ANSYS. The influence of the realistic situation including load and temperature on the residual stress of the coatings is investigated. Simulated results show that the realistic situation strongly affects the residual stress. To be specific, i) The main residual stress concentrates on the coatings prepared on YG8 substrate, and the residual stress and its gradient of the coatings are bigger than that of the substrate; ii) TiAlN and TiCN coatings have better resistance compression than that of TiN coatings in the same condition; iii) The improved multilayer structure of the gradient hard coatings produces weaker residual stress but higher anti-pressure of the substrate.

Key words: gradient coating, ANSYS, residual stress, hard coatings

0 Introduction

Hard coating materials have been widely used in mold manufacturing^[1], aero engine^[2], medical^[3], astrology^[4] and other fields for its excellent hardness, oxidation resistance, corrosion resistance, high temperature stability, electrical conductivity and smaller friction factor. However, due to the low bonding strength between hard coating and substrate, crack from the high residual stress caused by the load is generated at the interface, which makes the dies, tools or the devices failed. So, it is important to analyze the stress distribution law of the matrix and the coatings, the fracture strength of the crack, and the dynamic characteristic of the coating structure^[5,6].

Meanwhile, it is available and satisfied to solve the contact problem, which is difficult to obtain the exact solution of the coating materials by the numerical methods with the improvement of the computer performance. Coating/substrate bonding strength is an important index to study the coating performance, and the contact width is very important to investigate the bonding strength of the coating/substrate. The theory of the coating/matrix has achieved some success internationally. Gong and Qiao tested the residual stress curve of the TiN coating on HSS. The residual stress ranging

from 3.12GPa to 2.29GPa and thermal stress of the coatings ranging from 1.96GPa to 1.92GPa with the thickness from 3 μ m to 11 μ m were achieved by finite element analysis respectively^[7]. Gong, et al. designed the Y-TZP/LZAS glass ceramics function gradient coating, and analyzed the effect of gradient the coating/substrate interface residual stress on the composition distribution of the gradient index, layer number and layer thickness and other parameters using finite element software^[8]. Thanongsak, et al. studied the effect of cBN coating on the tool wear resistance by using the method of combining experiment and the finite element simulation, and reached that the tool with cBN coatings could reduce the wear rate and the cutting temperature of the tool^[9]. Zhang, et al. established a bonding interface stress detection system about coating, and researched on the interface state detection^[10]. However, there are very limited reports regarding the structure design of gradient hard coatings and the residual stress simulation.

The structure of Ti gradient hard coatings is designed, and the residual stress change at different working temperature and loading is analyzed by ANSYS, which provides a basis for improving the physical and mechanical properties of the gradient coatings and optimizes the structure design in this paper.

① Supported by the National High Technology Research and Development Programme of China (No. 2012AA09A203) and Project of Sichuan Education Department (No. 14ZA0321).

② To whom correspondence should be addressed. E-mail: 48055130@qq.com

Received on Aug. 23, 2016

1 Establishment and evaluation of the model

1.1 Creating and meshing the model

The substrate is YG8 with the length of 18mm and the radius of 8mm. The structure of the gradient coating is shown in Fig. 1

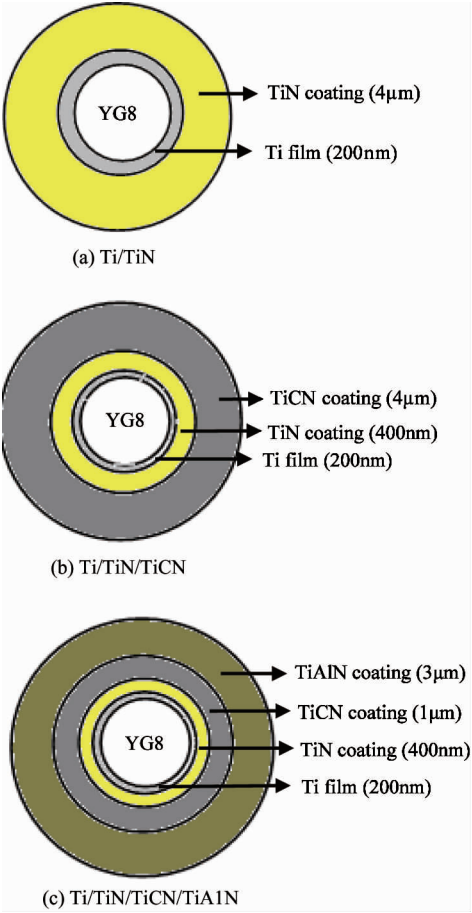


Fig. 1 Structure of the gradient coating in the simulation and calculation

The three-dimensional model of matrix YG8 and the hard coatings are established by ANSYS, and Fig.2 presents the establishment and mesh of the model. The substrate data and the coatings parameters from ANSYS are shown in Table 1. What’s more, the room temperature Young modules and Poisson ratio of YG8 are 210GPa and 0.28 , respectively. If the coating and the substrate can be seen as a whole, ignoring the influence of sliding friction on coating performance and alloy matrix, the effect of static pressure and different temperature on the residual stress of coating and substrate can be analyzed. The preparation technology of each coating is shown in Refs [11,12].

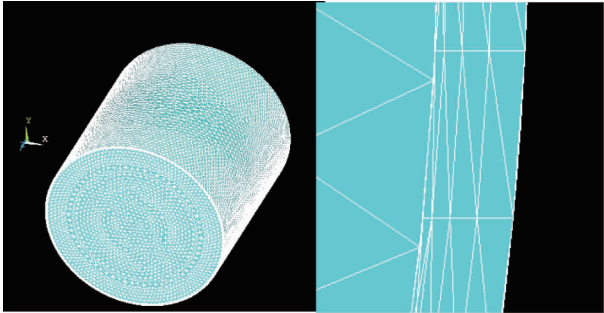


Fig. 2 Model of ANSYS simulation and calculation

The free meshing dividing is used. The different materials are gluing before free meshing dividing, and then loading and solving because the composite coatings are regarded as the different element.

The effect of cylindrical fretting pads on the substrate without coatings is used to estimate the finite element model for Hertz contact theory only applied to analyze the contact stress of the substrate without coatings. The positive stress from ANSYS calculation was identical to that from Hertz contact theory resolution (shown in Fig.3).

Table 1 Coatings parameters^[13-15]

Coating	Elastic module <i>E</i> (GPa)	Poisson ratio <i>ν</i>	Hardness <i>G</i> (GPa)	Density <i>P</i> (g/cm ³)	Tension strength <i>σ_b</i> (GPa)	Compressive strength (GPa)	Linear expansion efficient <i>α</i> (10 ⁻⁶ K)	Thermal conductivity <i>λ</i> (W/m · K)	Specific heat <i>c</i> (J/kg · K)
TiAlN	376	0.36	47.5	6.35	0.8	0.81	9.20	19.9	270
TiCN	205	0.34	48.9	4.47	0.9	0.98	9.56	19.2	380
TiN	341	0.33	45.5	5.34	0.65	0.66	9.35	19.3	365
Ti	105	0.37	45.0	4.50	0.44	0.45	9.00	19.9	523

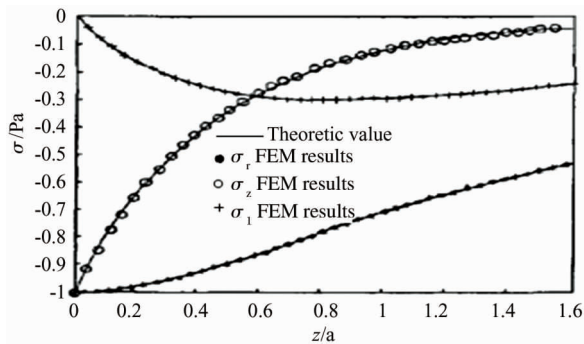


Fig. 3 Ratio of the stress theoretic value and numerical value of coatings model along front direction

1.2 Applying constrains, loading and solving

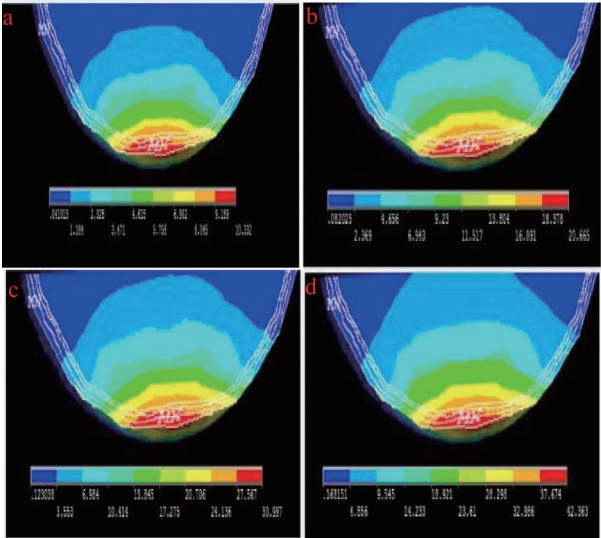
First, constrains are defined in order to apply load on the model. Changing mesh and studying the mesh-sensitivity are permitted on the solid model. And the procedure would transfer the loading of the solid to the finite model automatically.

On the other hand, temperature load and stress load are imposed on the material surface to study the influence of heat expansion and heat shrinkage on material stress and the influence of external stress on the residual stress of the material.

2 Results of analysis

2.1 Residual stress distribution when the YG8 substrate is combined with TiN/Ti coating

The distribution of residual stress of the coatings with the structure in Fig. 1 (a) is shown in Fig. 4 at the static loading of 100N, 200N, 300N, 400N at 25°C.



a:100N; b: 200N; c: 300N; d: 400N
Fig. 4 Residual stress nephogram of TiN/Ti coatings under different static loading at 25°C

It can be seen that the distribution of the residual stress of cemented carbide is different from the coating under different static loading. The residual stress concentrating on the local loading area of the coatings shows linear decrease between the area of coating and substrate. The stage of concentrated stress transferred to the gradient layer from the interface, which is benefit to avoiding material damage and mitigating external stress. So it enables the mould life to increase many times. To further research the distribution of residual stress in the direction of added stress, a coordinate system is established in which the abscissa is the distance from the surface to the outer layer and the ordinate is the inner residual stress as shown in Fig. 5.

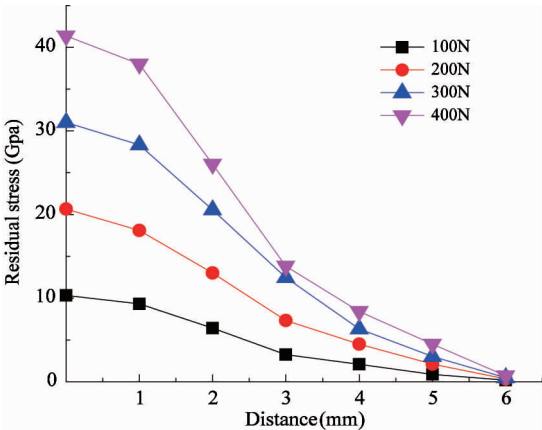
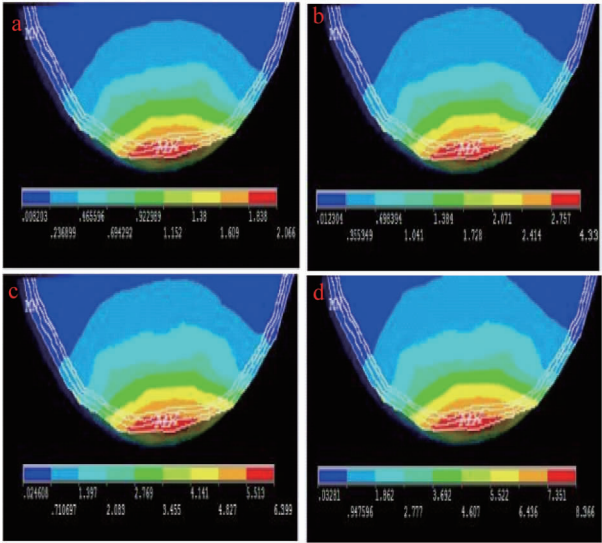


Fig. 5 Residual stress of TiN/Ti coatings under different static loading at 25°C

It can be seen that the residual stress of the sample decreased linearly, and the bigger the loading, the bigger the residual stress, the more damage of the coating. Meanwhile, the maximum of the residual stress 300GPa under the loading of 300N is close to the critical yield strength 20GPa^[16]. And the coating would be damaged seriously when the residual stress of the outer layer exceeds the conventional strength of the TiN coating to reach 42GPa under the loading of 400N. In conclusion, they provide instructive parameters to the application conditions of the gradient coating of the structure.

The distribution of residual stress of the coatings with the structure in Fig. 1 (a) is shown in Fig. 6 at 200°C, 400°C, 600°C, 800°C under 20N. It can be seen that thermal residual stress is different at the inhomogeneous temperature difference at the same loading. Moreover, it presents that the higher the temperature, the larger the residual stress in the coatings. Nonetheless the residual stress in the substrate increases a little for the insulation of ceramic coating reduces the input energy of the substrate. So the substrate temperature is

lower than that of the coating, and the rising rate of the residual stress is relatively small with the increasing of the heat loading. Meanwhile the residual stress curve of coatings from Fig.6 is shown in Fig.7. The establishment method of the coordinate system is similar to that of Fig.5.



a: 200℃ ; b: 400℃ ; c: 600℃ ; d: 800℃
Fig. 6 Residual stress nephogram of TiN/Ti coatings at different temperature under 20N

Fig.7 shows that the bigger temperature loading on the coating, the bigger the residual stress is and the lower of compression residence capability, which will cause more damage. Nonetheless it does not reach the strength limit of TiN coating when the residual stress reaches 10GPa at the working temperature of 800℃. On the other hand, it is significant to consider the influence of the high temperature oxidation resistance of TiN coating in practical applications^[17].

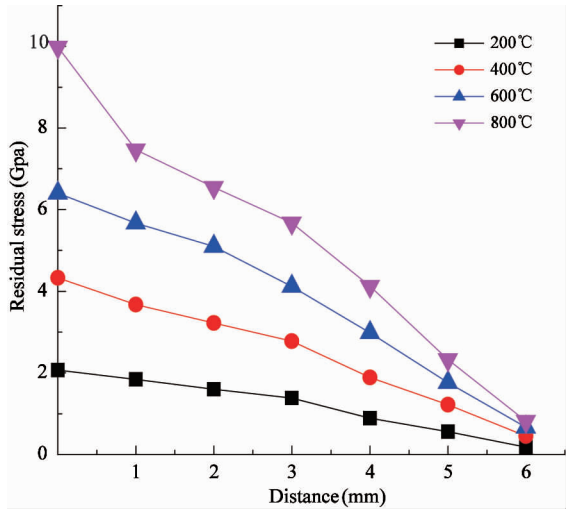
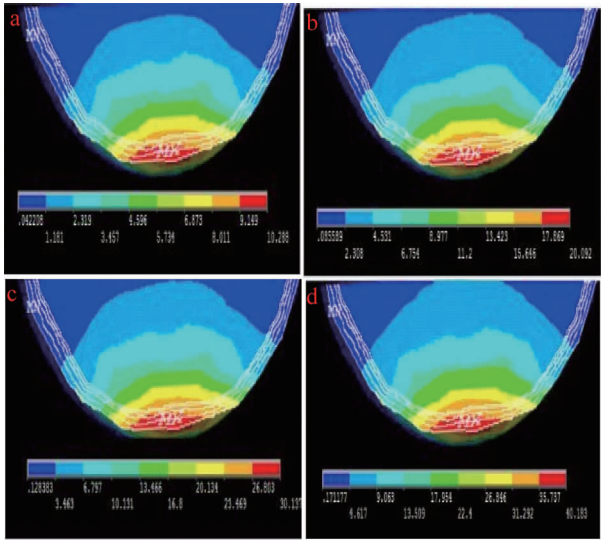


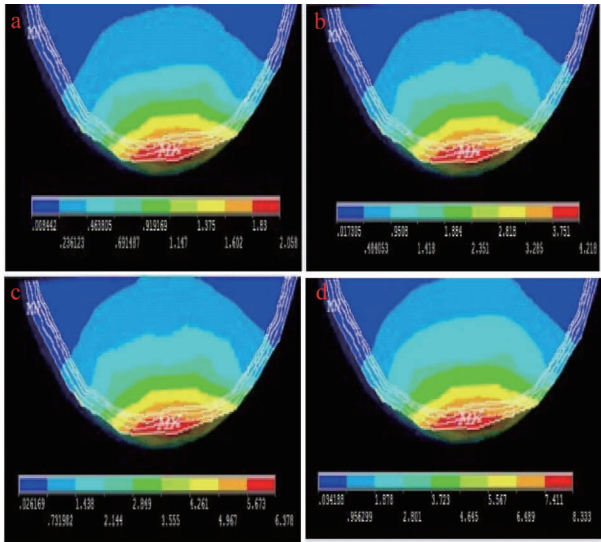
Fig. 7 Residual stress curve of TiN/Ti coatings at different temperature under 20N

2.2 Analysis of the binding stress between the YG8 substrate and TiCN/TiN/Ti coating

The nephogram of residual stress of the sample with the structure in Fig. 1 (a) under the different static loading and temperature is shown in Fig.8 and Fig.9. The distribution trend of the residual stress is the same as Fig.4 and Fig.6. The distribution curve of stress made method as the same as Fig.5 is shown in Fig.10 and Fig.11. Compared with Fig.5 and Fig.7, it can be concluded that the maximum of residual stress with the structure of in Fig. 1 (b) is less than that of the structure in in Fig. 1(a) under different loading at room temperature. What’s more, the yield strength of TiCN coating is bigger than that of TiN coating^[18]. In



a: 100N ; b: 200N ; c: 300N ; d: 400N
Fig. 8 Residual stress nephogram of TiCN/TiN/Ti coatings under different static loading at 25℃



a: 200℃ ; b: 400℃ ; c: 600℃ ; d: 800℃
Fig. 9 The residual stress nephogram of TiCN/TiN/Ti coatings at different temperature under 20N

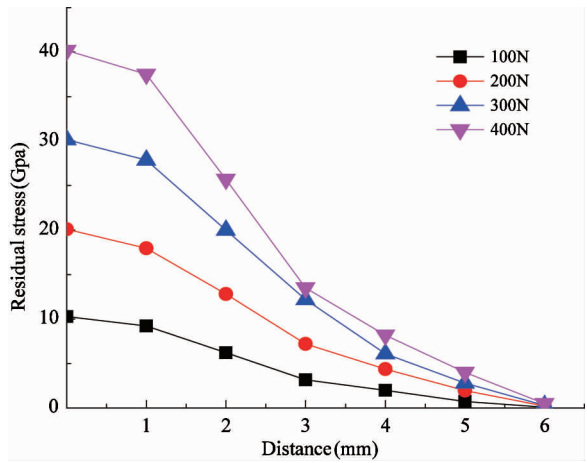


Fig. 10 Residual stress of TiCN/TiN/Ti coatings under different static loading at 25°C

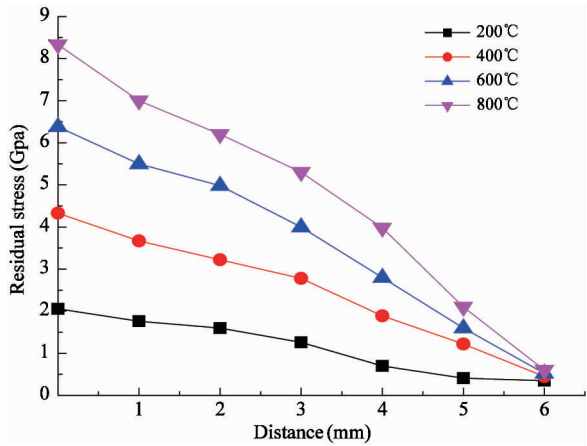


Fig. 11 Residual stress of TiCN/TiN/Ti coatings at different temperature under 20N

conclusion, the design of the gradient not only relieves the residual stress from the external loading, but also solves the contact problem of the materials with big hardness. Thus it improves the binding force of coating and substrate.

2.3 Analysis of binding stress between YG8 substrate and TiAlN/TiCN/Ti coatings

In order to further improve hardness of coating and binding force between hard coating and substrate, the structure of the gradient coating in Fig. 1 (c) is designed and prepared. Then the stress of the coating under different loading is simulated.

The nephogram of residual stress at different loading and temperature is shown in Fig. 12 and Fig. 13, respectively. The distribution curve of stress is shown in Fig. 14 and Fig. 15. It shows that the residual stress of

the coating is smaller than that of the coatings with the structure in Fig. 1 (a) or Fig. 1 (b) TiAlN coating has so high yield strength with 60GPa and high temperature oxidation resistance closed to 1000°C that the problem of binding force is solved between TiAlN/TiCN/TiN/Ti gradient coating and YG8 substrate easily^[19]. So it enables the mould life to increase many times when the simulated condition of gradient coating is used in practical applications.

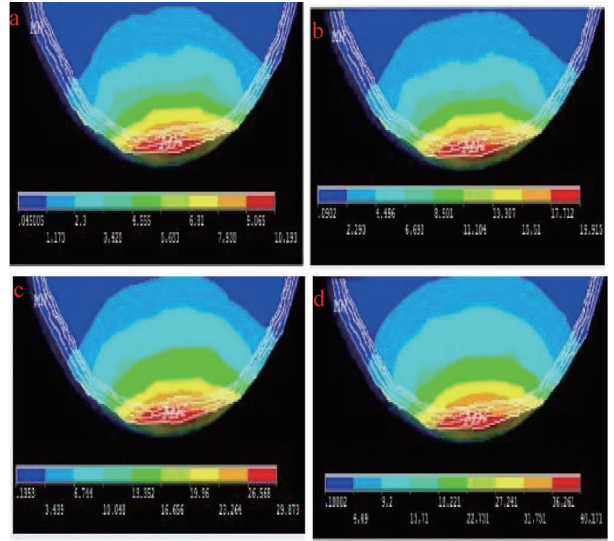


Fig. 12 Residual stress nephogram of TiAlN/TiCN/TiN/Ti coatings under different static loading at 25°C

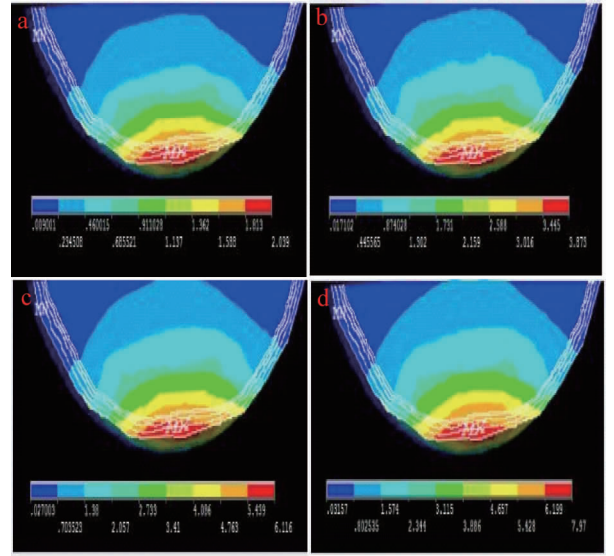


Fig. 13 Residual stress nephogram of TiAlN/TiCN/TiN/Ti coatings at different temperature under 20N

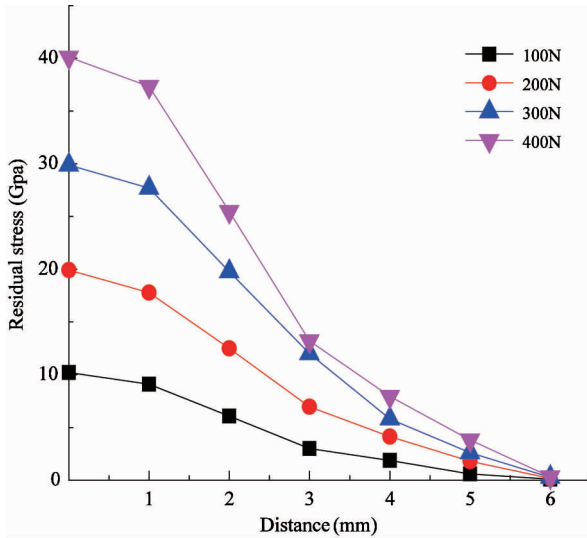


Fig. 14 Residual stress of TiAlN/TiCN/TiN/Ti coatings under different static loading at 25°C

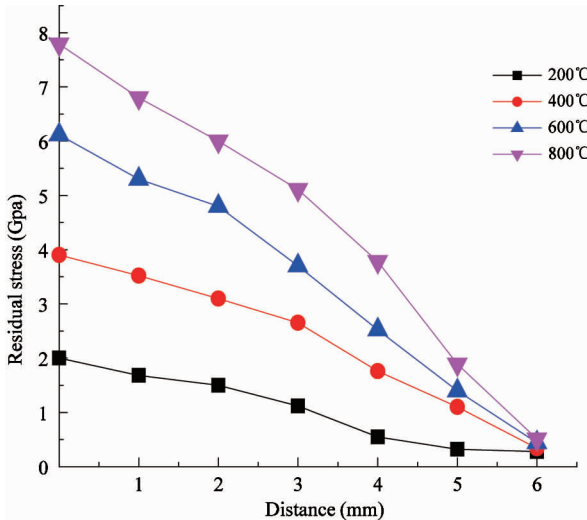


Fig. 15 Residual stress of TiAlN/TiCN/TiN/Ti coatings at different temperature under 20N

3 Conclusions

(1) The main residual stress concentrates on the coatings prepared on the YG8 substrate, and the residual stress and its gradient of the coatings is bigger than that of the substrate.

(2) The compressive performance of TiAlN coating is better than that of TiCN coating under the same condition, and the TiAlN coating can increase the life of the substrate.

(3) With the increasing of the layer number of the gradient coating and the improvement of the structure, it not only solves the problem of the binding force between hard coatings and substrate, but also decreases the residual stress of the coating and the substrate under the external loading.

Reference

- [1] Gill S S, Singh H, Singh R S J. Processing of cutting tool materials—a review. *International Journal of Advanced Manufacturing Technology*, 2010, 48(1-4):175-192
- [2] Shum P W, Li K Y, Zhou Z F. Structural and mechanical properties of titanium-aluminium-nitride films deposited by reactive close-field unbalanced magnetron sputtering. *Surface & Coatings Technology*, 2004, 185(2-3):245-253
- [3] Li L, Zhao J, Gu H Q. Study on the biocompatibility of titanium nitride ceramic films by ion beam assisted deposition. *Chinese Journal of Dialysis and Article Organs*, 2003, 14(3):1-6 (In Chinese)
- [4] Takalka H, Nakamura E, Oshika T, et al. Relationship between an affinity of $(\text{Ti}_{1-x}\text{Al}_x)\text{N}$ layer toward iron and its cutting performance. *Surface & Coatings Technology*, 2004, 177-178:306-311
- [5] Kim C H, Perkins N C, Lee C W. Parametric resonance of plates in a sheet metal coating process. *Journal of Sound and Vibration*, 2003, 268(4):679-697
- [6] Hang L X, Yin Y, Xu J Q. Optimization of diamond-like carbon films by unbalanced magnetron sputtering for infrared transmission enhancement. *Thin Solid Film*, 2006, 515(1):357-361
- [7] Gong M F, Qiao S R, Lu G F. Curvature testing and finite element analysis for the residual stresses in TiN coatings on high speed steel. *Journal of Mechanical Engineering*, 2010, 46(6):100-106 (In Chinese)
- [8] Gong W, Zhou L M, Wang E Z. Finite element analysis of residual stresses on Y-TZP/LZAS glass-ceramic gradient Coatings. *Chinese Journal of Materials Research*, 2014, 28(10):787-793 (In Chinese)
- [9] Thanongsak T, Tugrul O. Experimental and finite element simulation based investigations on micro-milling Ti-6Al-4V titanium alloy: Effects of cBN coating on tool wear. *Journal of Materials Processing Technology*, 2013, 213(4):532-542
- [10] Zhang Y K, Kong D J, Feng A X. Study on the detection of interfacial bonding strength of coatings (II): detecting system of bonding strength. *Acta Physica Sinica*, 2006, 55(11):6008-6012 (In Chinese)
- [11] Song H J, Yan Q. The characteristics of CrNx coatings with different interlayer. *Advanced Materials Research*, 2011, 204-210:938-941
- [12] Song H J, Yan Q. Growth and property characterization of Ion plated $\text{Ti}_{1-x}\text{Al}_x\text{N}$ coating. *Chinese Journal of Vacuum Science and Technology*, 2013, 33(1):61-67 (In Chinese)
- [13] Chen R, Tu J P, Liu D. Microstructure, mechanical and tribological properties of TiCN nanocomposite films deposited by DC magnetron sputtering. *Surface & Coatings Technology*, 2011, 205(21):5228-5234

- [14] Thomas R, David G S, Valeriu C. Structure and mechanical properties of TiAlN - WN_x thin films. *Surface & Coatings Technology*, 2011, 205(20):4821-4827
- [15] Zhou Y X, Zhu X F, Zhang J J. Microstructure and cutting performance of TiCN and TiN tooling coatings prepared by ion plating. *Tool Technology*, 2010, 44(11): 18-21 (In Chinese)
- [16] Liu Y F, Zhang G L, Wang J L. Preparation of titanium nitride films by pulsed high-energy-density plasma and investigation of the tribological behavior of the film. *Acta Physica Sinica*, 2004, 53(2): 503-507 (In Chinese)
- [17] Chen X M, Yi D Q, Huang D Y. Thermal oxidation resistance of TiN/TiCN/Al₂O₃/TiN multilayer coatings on cemented carbide by chemical vapor deposition. *The Chinese Journal of Nonferrous Metals*, 2011, 21(8): 1967-1973 (In Chinese)
- [18] Wang L, Zhang J, Xue Q, et al. Microstructure and friction & wear behavior of TiC/Ti (C_xN_{1-x})/TiN coating. *Materials Protection*, 2013, 46(5):54-57
- [19] Braic M, Braic V, Balaceanu M, et al. Synthesis and characterization of TiN, TiAlN and TiN/TiAlN biocompatible coatings. *Surface & Coatings Technology*, 2005, 200(1-4):1014-1017

Song Huijin, born in 1978. She received her Ph. D and M. S. degrees in Materials Science Department of Sichuan University in 2009 and 2006 respectively. Her research interests include the hard coatings, thin films materials and device.